Study on Performance of Flame Retardant and Smokeless Reed/Magnesite Cement Inorganic Particleboard

Xia Zheng
Peiqi Li
Yunfei Lin
Xingong Li

Abstract

Flame-retardant reed inorganic particleboard was prepared by hot-pressing with reed particles as a reinforcing material and using magnesite cement as an inorganic adhesive. The effects of inorganic sizing amount, density, and hot-pressing temperature and time on the properties of reed inorganic particleboard were investigated by orthogonal testing. Particleboard properties were tested and characterized by means of a universal mechanical testing machine, scanning electronic microscopy (SEM), X-ray diffraction (XRD), and cone calorimetry. The results showed that the mechanical properties of particleboard prepared under conditions of 60 percent sizing capacity, 100°C hot-pressing temperature, 15 minutes hot-pressing time, and 1.2 g/cm^3 density were the best, reaching the national standard for cement particleboard. At 60 percent sizing, the characteristic peak value of inorganic adhesive hydrate crystal phase was the largest, the crystallization area dense and orderly, and the coating effect on shavings good; these attributes confirmed the trend of mechanical properties of reed shavings board increasing with sizing amount. Thus, the sizing amount had a significant influence on flame retardancy and smoke suppression performance of this particleboard. With an increased application amount, the heat release and total heat release rates of the particleboard and total smoke generation rate showed decreasing trends. Additionally, when the ignition time was delayed, the flame retardancy and smoke suppression performance of the particleboard was enhanced.

At present, the main raw materials of particleboard are relatively common biomass materials, such as wood, bamboo, and agricultural and forestry residues (Zhang et al. 2013, Atoyebi et al. 2018, Farag et al. 2019). Its strength is moderate, the structure even, and processing performance good. It also has good sound absorption and insulation, is adiabatic and low cost, so it had many uses in furniture and interior decoration applications. However, burning particleboard is prone to smoke production, which causes serious casualties and property losses every year. In view of this problem, much research has been directed at the preparation of flame retardant particleboard.

Lan et al. (2015) and Chen et al. (2016) chose an inorganic compound flame retardant composed of aluminum hydroxide and zinc borate to produce flame-retardant straw particleboard; however, this inorganic flame retardant has only a general flame-retardant effect and the production process is tedious and thus not conducive to popularization of production. Pang and Yu (2016) have prepared aldehyde-free flame-retardant particleboard with flame-retardant soybean protein adhesive. However, the waterproof property of the soybean protein adhesive is poor. Fu (2012) and Fu et al. (2015) have prepared phosphorus, nitrogen, and boron flame retardants and studied their effects as flame retardants in particleboard. However, the production processes using these flame retardants are complicated, the resulting product mechanical properties are poor, and thus they do not meet market demand. China has become the world's largest

The authors are, respectively, Associate professor (zhengxia813@126.com [corresponding author]), postgraduate (632452396@qq.com), postgraduate (yunfeilinwood@163.com), professor(lxgwood@163.com), Central South Univ. of Forestry and Technol., Changsha, Hunan, China. This paper was received for publication in September 2020. Article no. FPJ-D-20-00051.

Forest Prod. J. 71(3):224–232.
doi:10.13073/FPJ-D-20-00051

country for wood-based panels, but the shortage of raw materials has become a bottleneck and restricted development of wood-based panels (Widyorini et al. 2016). Reeds are tall aquatic grasses with tough stems and high fiber content (~40%). Compared with other raw materials, reeds have longer fiber length and greater toughness, making them high-quality raw materials for wood-based panels (Zhang et al. 2015). China is rich in reed resources, with an area of $>1.3 \times 106$ hm^2 (Wang et al. 2006). The shortage of raw materials for wood-based panels can be alleviated by making better use of reed resources (Peng et al. 2017, Benthien et al. 2018). There is a waxy layer on reed surfaces, so it is difficult to use a common adhesive to produce a useful particleboard (Hafezi et al. 2016). Magnesium oxychloride cement is a kind of air-hardened cement that has good interfacial compatibility with reed shavings and is also fast-curing and has high strength. Moreover, magnesium oxychloride cement has excellent flame-retardant performance. Using magnesium oxychloride cement as the adhesive can achieve the integration of flame retardancy and adhesion; it also gives the board (plate) strength and provides flame retardant and smoke suppression performance. This could greatly improve production convenience, which is conducive to mass production.

The main purpose of this study is to prepare a kind of reed inorganic particleboard which is made of reed particle with low utilization rate as the main raw material and magnesite cement as inorganic adhesive and flame retardant. We used a hot-pressing forming process, which requires no aldehyde; this process is better for the environment and results in excellent flame retardant and smoke suppression properties. The influence of preparation process on its mechanical properties and flame retardant and smoke suppression properties was studied to provide reference for reed inorganic particleboard. The development of the particleboard provides theoretical and technical support for readers' reference.

Experimental Materials and Methods

Raw materials

Magnesium oxychloride cement, an inorganic adhesive, was prepared in the laboratory. Raw materials included lightly burned, industrial grade magnesium oxide (MgO) that contained 88 percent MgO, 2 percent CaO, 1.5 percent Fe_2O_3, and 4 percent losses by burning. Industrial grade hexahydrate magnesium chloride ($MgCl_2 \cdot 6H_2O$) was obtained from Sinopharm Group Chemical Reagent Co., Ltd. (China). Reed material was derived from annual fresh reed, from the Dongting Lake District.

Preparation of reed inorganic particleboard

The preparation process of reed inorganic particleboard in this study is shown in Figure 1. Appropriate amounts of magnesium sulfate, magnesium oxide, and magnesium chloride were dissolved into a fixed amount of water at a predetermined proportion and stirred with a glass rod for 3 minutes to obtain a milky white, viscous, inorganic adhesive. A weighed amount of reed shavings were placed in a blender, and the adhesive added according to set proportions of sizing amount, and stirred for 10 minutes. The mixed reed shavings were evenly spread in a 300 × 300-mm wooden molding frame and manually prepressed. The resulting slab was then hot-pressed and the formed plate thickness set to 8 mm by using a thickness gauge After hot-pressing, the plate was taken out and placed in a sealed bag for natural curing for 21 days. Finally, according to National Standard GB/ T 24312-2009, the plates were placed in an electric blast-drying oven and dried at 100°C until the moisture content was 10 percent.

Test scheme

The fixed parameters of reed inorganic particleboard included the following: 8 percent water content, a board surface size of 300 × 300 × 8 mm, glue mixer speed of 200 revolutions/min, 10 minutes stirring time, 5 MPa thermal pressure, and 21 days curing time.

In this experiment, an orthogonal design at four factors and three levels was adopted. The sizing amount, as the mass ratio of inorganic adhesive to total mass, was set at 50, 55, and 60 percent, with resulting densities of 1, 1.1, and 1.2 g/cm^3, respectively. The hot-pressing temperatures were 90°C, 100°C, and 110°C, and hot-pressing times at 15, 20, and 25 minutes (Tables 1 and 2).

Performance testing and characterization

According to GB/T 24312-2009, the mechanical properties of the present square plate samples were tested. The static bending strength (MOR), elastic modulus (MOE), water absorption thickness expansion rate (TS), and internal bonding strength (IB) of the squares were tested using a BY302X2/2 universal mechanical testing machine (Mattes Industrial Systems Co., Ltd., China) Three specimens were used in each test and the average taken.

X-ray diffraction (XRD) detection.—After a specimen was completely broken and finely ground, a 200-mesh fine sieve was used to refine the powder sample, and an XD-2 X-ray diffractometer (PERSEE Analytics, Inc., USA) was used for analysis, with 36-kV voltage, 20-mA current, a Cu-Kα target (0.154 nm), scanning speed 2 at 4°/min, and scanning range of 5° to 75°.

Table 1.—Factors and levels table of orthogonal test.

	Factors			
Level	Resin content (A; %)	Hot-pressing temperature (B; °C)	Hot-pressing time (C; min)	Density (D; g/cm^3)
1	50	90	15	1.0
2	55	100	20	1.1
3	60	110	25	1.2

Table 2.—Mix ratio of orthogonal test.

Number	Resin content (A; %)	Hot-pressing temperature (B; °C)	Hot-pressing time (C; min)	Density (D; g/cm^3)
1	50	90	15	1.0
2	50	100	20	1.1
3	50	110	25	1.2
4	55	90	20	1.2
5	55	100	25	1.0
6	55	110	15	1.1
7	60	90	25	1.1
8	60	100	15	1.2
9	60	110	20	1.0

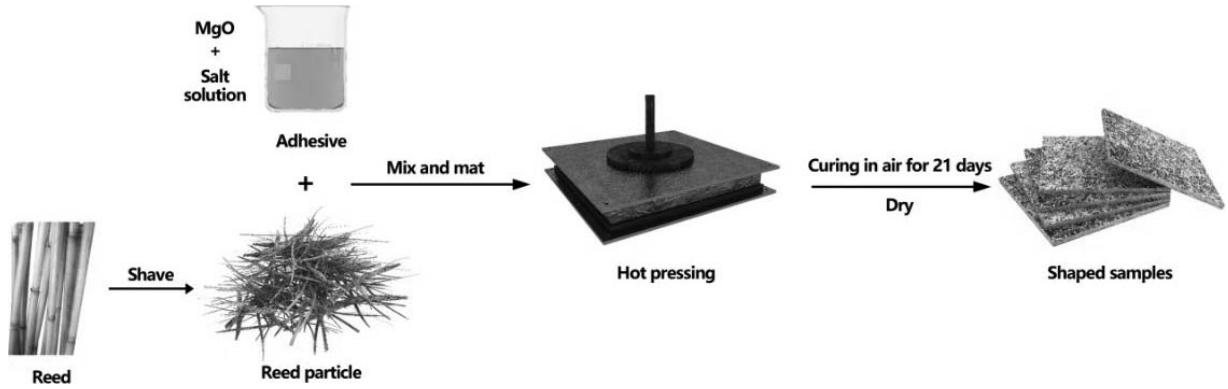

Figure 1.—Flow chart for preparation of reed inorganic particleboard.

Cone calorimeter detection.—An FTT007 conical calorimeter of (Fire Testing Technology, UK) was used to conduct combustion experiments on 100 × 100-mm specimens, with the radiation power at 50 kW/m^2 (the surface temperature of composite material under this radiation power was ~780°C).

Results and Discussion

The MOR, MOE, TS, and IB of reed inorganic particleboard were obtained according to the Table 2 orthogonal test mix ratio (Table 3).

Analysis of mechanical properties

Each index was calculated and analyzed individually, and then the analysis results of each index were balanced to obtain the best test scheme. As shown in Table 3, the experimental values (K) for each factor were calculated, and the values of the group mean (K_n, n = 1,2,3...) and range (R) were obtained (see Tables 4–10 for details).

Range analysis results of MOR and MOE.—In Table 4, A is the sizing amount, B the hot-pressing temperature, C the hot-pressing time, and D the thermal pressure temperature. The range analysis of MOR and MOE in Table 3 is carried out, and the analysis results are shown in Table 4. It can be seen from table 4 that the primary and secondary factors affecting the MOR of reed–inorganic adhesive particleboard are C > A > D > B. The hot pressing time has the greatest influence on the MOR, followed by the sizing amount, the density and the hot pressing temperature.

In order to intuitively observe the influence of various factors on the static bending strength of plates, the horizontal

Table 3.—Test results of mechanical properties. MOR is modulus of rupture; MOE is modulus of elasticity, TS is thickness swelling; and IB is internal bonding moment.

Number	MOR (MPa)	MOE (MPa)	TS (%)	IB (MPa)
1	10.5	1,596	20.50	0.24
2	11.1	1,868	13.30	0.48
3	8.7	1,144	14.70	0.42
4	16.6	2,656	13.50	0.49
5	10.9	1,652	10.10	0.34
6	17.1	2,938	8.20	0.33
7	11.1	1,832	12.40	0.46
8	22.2	3,608	9.10	0.59
9	15.0	2,472	5.40	0.21

Table 4.—Modulus of rupture/modulus of elasticity (MOR/MOE) range analysis results.

	MOR (MPa)				MOE (MPa)			
Number	A	B	C	D	A	B	C	D
K1	10.1	12.73	16.6	12.13	1,536.00	2,028.00	2,714.00	1,906.67
K2	14.87	14.73	14.23	13.1	2,415.33	2,376.00	2,332.00	2,212.94
K3	16.1	13.6	10.23	15.83	2,637.33	2,184.67	1,542.67	2,469.81
R	6	2	6.37	3.7	1,101.33	348.00	1,171.33	562.14

Table 5.—Variance analysis results of modulus of rupture. Asterisk indicates significance.

Sources of variance	SS[a]	f[b]	F[c]	$F_{critical}$	Saliency
A	60.242	2	1.601	4.460	*
B	6.036	2	0.160	4.460	
C	62.136	2	1.651	4.460	
D	22.096	2	0.587	4.460	
Error	150.510	8			

[a] Sum of squares of mean deviation.
[b] Free degree.
[c] Mean square ratio.

Table 6.—Variance analysis results of modulus of elasticity. Asterisk indicates significance.

Sources of variance	SS[a]	f[b]	F[c]	$F_{critical}$	Saliency
A	2,035,446.220	2	1.684	4.460	*
B	182,256.890	2	0.151	4.460	
C	2,140,992.890	2	1.771	4.460	
D	476,107.560	2	0.394	4.460	
Error	4,834,803.560	8			

[a] Sum of squares of mean deviation.
[b] Free degree.
[c] Mean square ratio.

Table 7.—Range analysis results of thickness swelling.

Number	A	B	C	D
K1	12.23	10.70	9.73	9.73
K2	9.37	9.53	8.80	9.33
K3	7.10	8.47	10.17	7.34
R	5.13	2.23	1.37	2.39

Table 8.—Variance analysis results of thickness swelling. Asterisk indicates significance.

Sources of variance	SS[a]	f[b]	F[c]	F critical value	Saliency
A	39.710	2	4.736	4.460	*
B	7.487	2	0.894	4.460	
C	2.927	2	0.232	4.460	
D	0.260	2	0.971	4.460	
Error	50.380	8			

[a] Sum of squares of mean deviation.
[b] Free degree.
[c] Mean square ratio.

Table 9.—Range analysis results of internal bonding strength.

Number	A	B	C	D
K1	0.360	0.397	0.387	0.263
K2	0.432	0.470	0.393	0.423
K3	0.511	0.330	0.407	0.500
R	0.151	0.140	0.020	0.237

axis and the static bending strength as the vertical axis were used to draw the trend chart of the influence of different levels on the static bending strength (Fig. 2).

When the hot-pressing time increased from 15 to 25 minutes, the MOR decreased by 38.37 percent and MOE decreased by 43.18 percent. The effect of hot-pressing time on static bending strength of plate is very significant because, with extended hot-pressing time, thermal stress accumulation inside the square increased and water loss intensified. During the natural curing period, the hydration reaction of the adhesive was insufficient and continuous glued interfaces did not form, resulting in decreased MOR (Zhang 2012). With the glue quantity (sizing) increased from 50 to 65 percent, the particleboard of MOR and MOE consequently increased with the greater numbers of hydration reaction sites. The hydration products formed a continuous bonding interface, reed shavings formed effective cladding, and the plate external collapse load capacity was enhanced. When the density increased from 1 to 1.2 g/cm^3, the plate MOR also increased accordingly because the plate density increased and the porosity decreased (Huang et al. 2008). This increased the contact area between the reed shavings and inorganic adhesives, forming a tightly bonded interface network and enhancing the plate MOR. Therefore, according to the static flexural strength trend diagram of different horizontal factors, the optimal horizontal combination of static flexural strength factors was A3B2C1D3.

Table 10.—Variance analysis results of internal bonding strength. Asterisk indicates significance.

Sources of variance	SS[a]	f[b]	F[c]	F critical value	Saliency
A	0.063	2	3.495	4.460	
B	0.026	2	1.030	4.460	
C	0.050	2	0.198	4.460	
D	0.093	2	5.201	4.460	*
Error	0.232	8			

[a] Sum of squares of mean deviation.
[b] Free degree.
[c] Mean square ratio.

Variance analysis of MOR and MOE.—Variance analysis was performed on MOR and MOE (Table 3) and the results shown in Tables 5 and 6. Find out the critical value f from the F distribution table α, The value of F calculated in ''calculate F ratio'' is compared with the critical value. If $F > F_{critical}(F\alpha)$, it indicated that this factor had a significant influence on the test result. The larger the difference between the two values, the greater the significance of this factor. If the influence of all factors on the index was not significant, the order of influence was determined by looking directly at the size of the F ratio and the following judgment the same. No factor was seen to be the most significant factor affecting the MOR of the plate bonding strength; however, the influence of all factors on MOR and MOE was consistent, with the influence from most to least being hot-pressing time, sizing amount, density, and hot-pressing temperature.

Range analysis of expansion rate of water absorption thickness.—Range analysis was conducted using the expansion rate of water absorption thickness shown in Table 3, and the analysis results are shown in Table 7. The order of primary and secondary factors affecting the expansion rate of sheet water absorption thickness was A

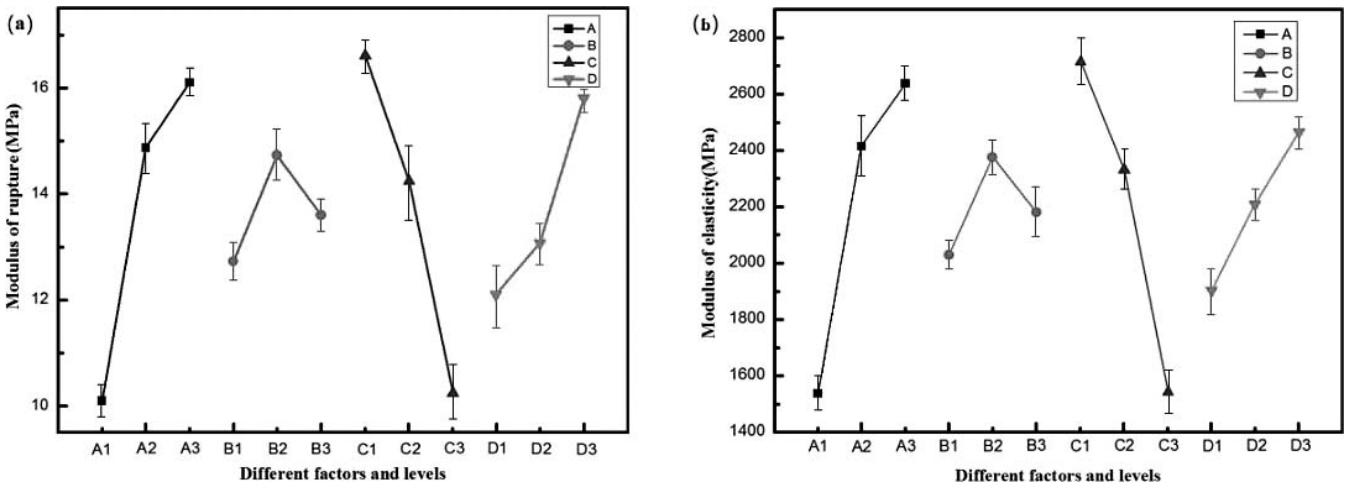

Figure 2.—Trend charts of mechanical properties of different factors and levels.

> D > B > C. The sizing amount had the greatest influence on the expansion rate of sheet water absorption thickness (TS), followed by density and hot-pressing temperature, and finally hot-pressing time. To illustrate the influence of different factors on the TS, the data were plotted in Figure 3.

The sizing amount had the greatest effect on the TS. When the sizing amount increased from 50 to 60 percent, the board TS decreased by 41.95 percent because, on one hand, the reed shavings were a porous material with the characteristics of dry shrinkage and wet expansion. With inorganic adhesive, the hydration reaction increased and reed particle proportion decreased; these factors also decreased water absorption performance because the adhesive coated the reed shavings and less moisture easily moved into reed pores. On the other hand, magnesium oxychloride cement has resistance to water, so the magnesium oxychloride cement hydration products produced by crystallinity were more abundant and thus the waterproof performance better. The optimal factor level influencing panel TS was selected as A3B3C2D3.

Variance analysis of the expansion rate of water absorption thickness.—Variance analysis was performed on TS using the values shown in Table 3 and the results are shown in Table 8. The F of the sizing amount was the largest and the significant factor influencing TS. The $F < F_{critical}$ of the other factors were considered to have no significant influence on the MOE. The significant effects of various factors on TS were sizing amount, hot-pressing temperature, density, and hot-pressing time.

Range analysis of internal bonding strength.—The range analysis of IB using the values shown in Table 3 was carried out and the analysis results are shown in Table 9. The primary and secondary factors influencing plate IB were D > A > B > C. The density had the greatest influence on the bonding strength. It could be said that particleboard density determined many physical and mechanical properties. Within a certain range, with increased plate density, the related mechanical properties also increased. The effect of sizing amount and hot pressing temperature on the internal bond strength of sheet is the second, and the effect of hot pressing time on the internal bond strength of sheet is the least. (Fig. 4).

The greatest effect of plate density on the IB can be seem from the three levels of growth, with the plank of IB

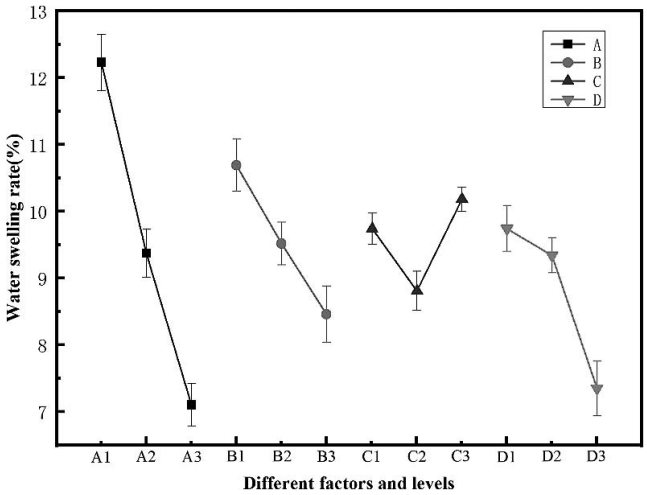

Figure 3.—Water absorption thickness expansion rate (TS) treatment charts of different factors and levels.

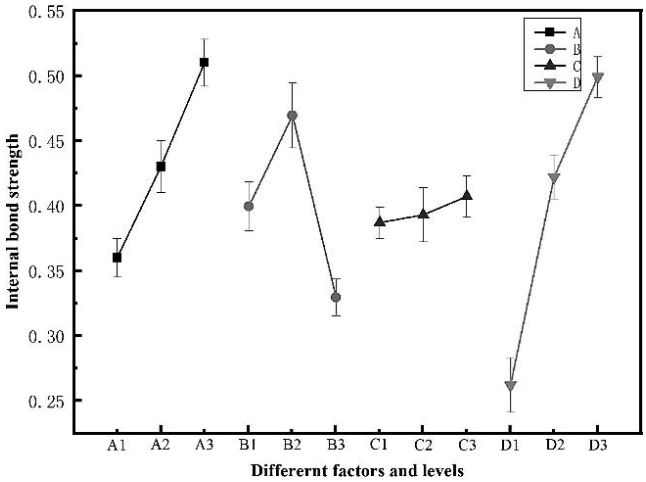

Figure 4.—Internal bonding strength (IB) treatment charts of different factors and levels.

increasing by 90.11 percent. The reason for this phenomenon is that with the increase of density and constant volume, the density of the density of the initial plate increases gradually, the porosity inside the density of the initial plate decreases gradually, the connection points of the gluing interface increase, the interface strength increases, and the ability to resist external damage load increases. Additionally, as the density increases, the quality of reed shavings and inorganic adhesives as the base material increases correspondingly; both factors play a role in enhancing the mechanical strength of the plate. With increased sizing amount, the IB also tended to increase because, with increased inorganic adhesive, hydration reaction products increased and shavings bonded more firmly, which gradually increased the IB. However, with increased hot-pressing temperature, plate IB first increased and then decreased (Yang and Li 2019). This was because hydration reactions were accelerated in a certain range with increased temperature, making the reaction more than sufficient and generating more hydration products. When the temperature is too high, the sheet forming under high steam pressure is subject to steam impact, plate initial internal moisture moving outward, water erosion, reed rod surface wax layer (Wang et al. 2013), reed stems of high ash content, and a higher percentage of SiO_2 of ash (Zhou et al. 2015). Also, the hydration reaction is not complete and cannot produce enough adhesive material, such that reed surface performance is poorer and agglutination performance bad, resulting in decreased IB. Here, the optimal factor level influencing plate IB was selected from Figure 4 as A3B2C3D3.

Analysis of variance of internal binding strength.—Density had the most significant effect on the IB, such that, as density increased, the bonding strength in plates increased. When the density increased from 1 to 1.2 g/cm^3, the plate IB increased by 90.11 percent. The two factors that had the greatest influence on the plate bonding strength were density and sizing amount, which were also confirmed by the factors influencing TS (Table 10).

Scanning electron microscopy (SEM) analysis.—Figure 5 shows the SEM comparison of reed inorganic particleboard under different sizing amounts. The area of hydration reaction is relatively dispersed as a result of adding large

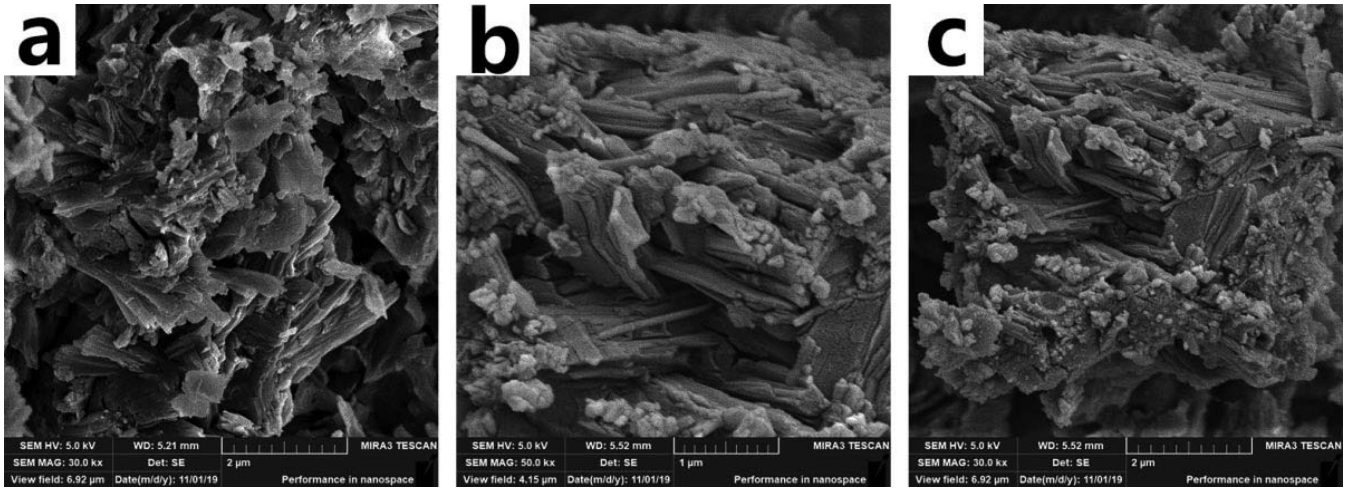

Figure 5.—Scanning electronic microscopy (SEM) diagram comparison of plates with different sizing amounts—50, 55, and 60 percent sizing amount, respectively (a–c).

amounts of reed shavings, and the resultant crystallization particles f are small with poor mechanical properties (Fig. 5a). Compare this with Figure 5a, where crystal size in plates increased significantly with increased sizing. This indicated that the reaction zone of hydration reaction increased with increased sizing, such that better crystallization effects were obtained. This comparison also showed that, with increased crystallization, reed material near the crystallization was combined with the crystallization in an orderly and dense manner, forming stronger glue interfaces, such that the mechanical properties of the plates were significantly improved. Finally, when the sizing amount reached 60 percent, the hydration reaction crystals were large and orderly and reed fibers tightly wrapped in the crystallization area, showing a very good binding effect (Fig. 5c). This was consistent with the mechanical properties analyzed above.

X-ray diffraction analysis

X-ray diffraction patterns of reed inorganic particleboard with different sizing amounts revealed that the main crystalline phases in the magnesium chloride cement products were $3Mg(OH)_2{\cdot}MgCl_2{\cdot}8H_2O$ (phase 318) and $5Mg(OH)_2{\cdot}MgCl_2{\cdot}8H_2O$ (phase 518; Zhou et al. 2015). The reactions were as follows:

$$MgO + H_2O \leftrightarrow Mg_2 + +2OH_- \quad (1)$$

$$4Mg_2 + +2Cl_- + 6OH_- + 8H_2O \leftrightarrow 3Mg(OH)2 \cdot MgCl_2 \cdot 8H_2O \quad (2)$$

$$6Mg_2 + +2Cl_- + 10OH_- + 8H_2O \leftrightarrow 5Mg(OH)2 \cdot MgCl_2 \cdot 8H_2O \quad (3)$$

Phase 518 is the main phase that determines the mechanical properties and strength of magnesium oxychloride cement products. With the increase of the reaction time at this stage, the cement strength of magnesium oxychloride continuously increases, and phase 518 and phase 318 can be converted to each other (Hu et al. 2016). The positions of diffraction peaks from plates produced with different sizing amounts were basically the same, indicating that hydration products generated by the reaction of inorganic adhesives are basically the same under different sizing amounts. With increased sizing amount, the intensity of diffraction peaks corresponding to phase 518 gradually increased and was highest when the sizing amount was 60 percent. This was due to the increased amount of sizing, which allowed more hydration reactions to occur and generated more phase 518 hydration product, resulting in greater mechanical strength (Hu et al. 2016; Fig. 6).

Flame-retardant performance analysis

Analysis of heat release.—Examination of heat release rate (HRR) and total heat release (THR) curves of reed inorganic particleboard with different sizing amounts showed that the variation trends of plates with different

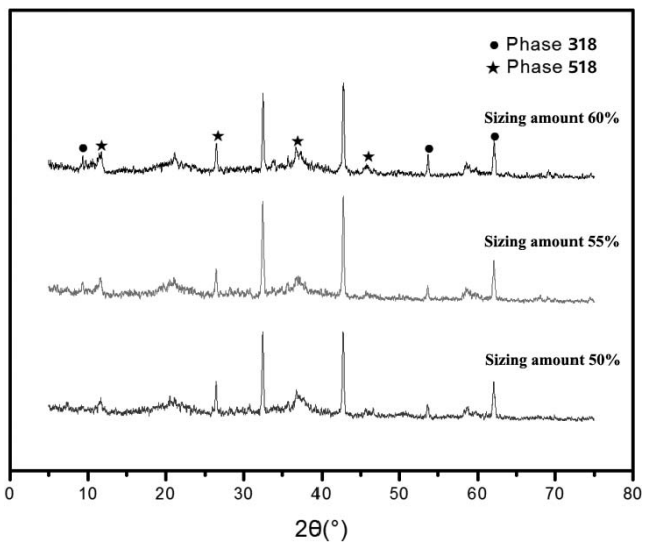

Figure 6.—X-ray diffraction (XRD) charts of reed plates with different gluing quantities.

sizing amounts were roughly the same. At 0 to 400 seconds, the HRR of the three kinds of plates showed a gentle growth trend, while at 400 to 800 seconds, they exhibited a sharp rise, reached a peak HRR, and then gradually declined because the adhesive played a major role in the flame retardant process (Zuo et al. 2018). When the temperature reached the burning point of the reed shavings, the inorganic adhesive decomposed, and the resulting magnesium oxide that attached to reed shaving surfaces delayed burning of the shavings (Zhu et al. 2008). The larger the sizing amount in the plate, the slower the HRR, the lower the maximum HRR, the less heat released per unit time, and the slower the combustion process. THR stability values of the three plates with different sizing amounts were 45.5, 38.4, and 17.7 MJ/m^2. With increased sizing amount, THR stability decreased significantly. The reason for this was that the inorganic adhesive was decomposed by heat into endothermic reactions (Xie 2008), producing HCl, H_2O, and MgO, and the generated water evaporated, removing heat, and lowering the plate temperature. At the same time, thermal decomposition of the inorganic adhesive consumed the oxygen around the plate, also delaying combustion. In addition, as the proportion of inorganic adhesives increased, the proportion of combustible reed shavings decreased, which reduced THR to some extent (Figs. 7, 8).

Flue gas release analysis.—Curves of the smoke produce rate (SPR) and total smoke production(TSP) of reed inorganic particleboard each had only one peak (Figs. 9 and 10, respectively). When the sizing amount was 50 percent, the smoke generation rate reached a peak of 0.0154 m^2/s at 65 seconds. At 55 percent sizing and 80 seconds, the peak was 0.0072 m^2/s. At 60 percent sizing, the peak was at 80 seconds and 0.0038 m^2/s. As a result of the increased amount of glue, hydration reactions that generated hydration products led to a corresponding increase in the amount of hydration products from thermal decomposition of the MgO type, including H_2O. With a more comprehensive reed shaving cladding, slowing of the spread of fire was better. The hydration reaction of magnesium hydroxide also had good smoke suppression

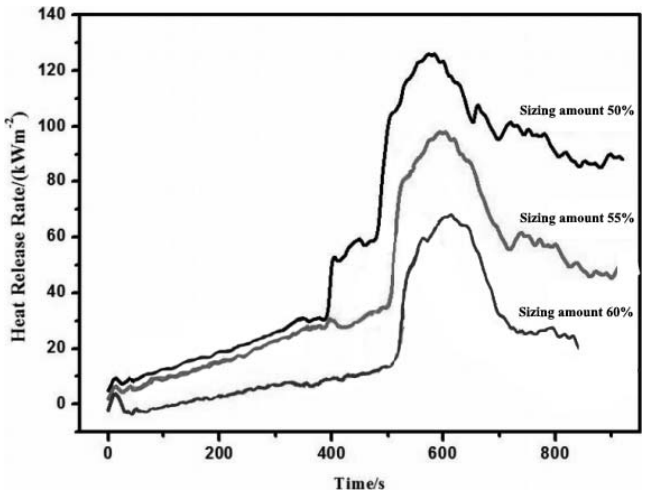

Figure 7.—Heat release rate (HRR) curves of reed board with different gluing quantities.

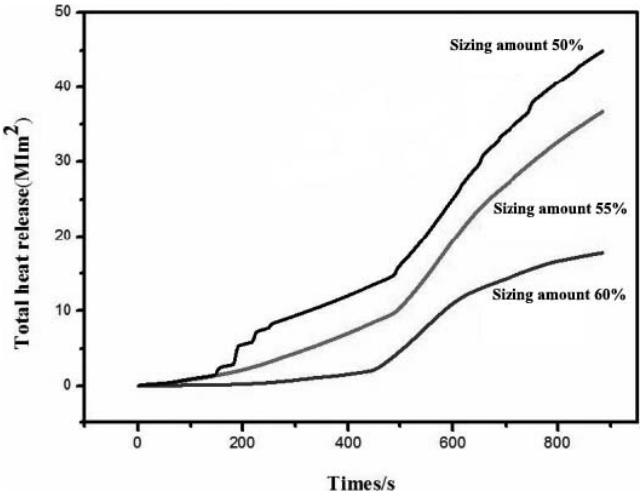

Figure 8.—Total heat release (THR) curves of reed board with different gluing quantities.

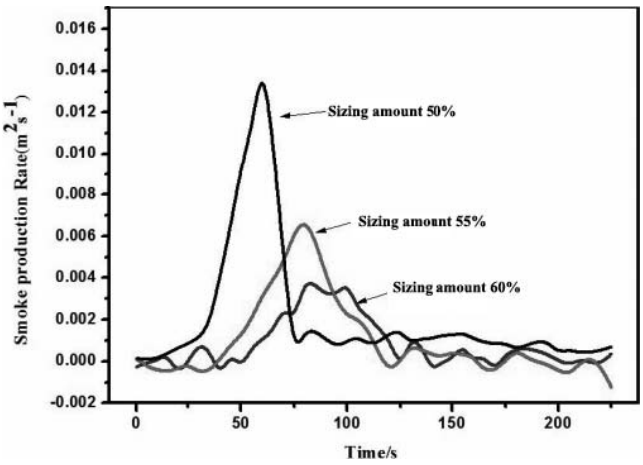

Figure 9.—Smoke produce rate (SPR) curves of particleboard with different gluing quantities.

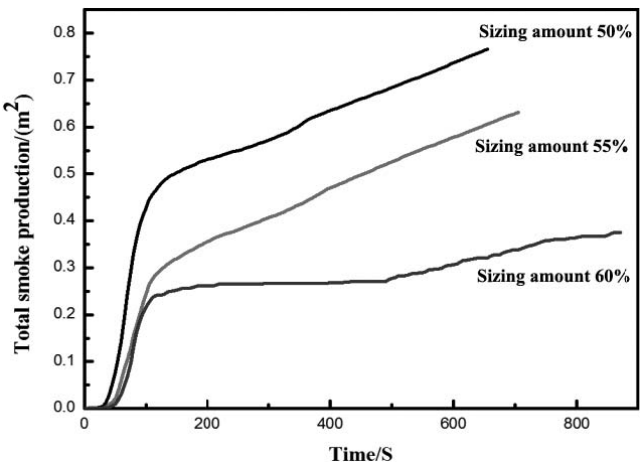

Figure 10.—Total smoke production (TSP) curves of reed board with different gluing quantities.

performance and could effectively adsorb of CO, CO_2, and other harmful smoke constituents. Thus, with sizing, the greater the amount of SPR in the later peak time, and the smaller the peak. The TSP with 55 and 60 percent sizing tended to be stable around 100 seconds, but with 50 percent sizing it continued to increase. These results occurred because, on one hand, the hydration reaction to produce magnesium hydroxide was an excellent flame retardant, which could also adsorb toxic smoke as a suppression function against flue gas. The more magnesium hydroxide produced by the hydration reaction, the better the flame retardant effect. On the other hand, magnesium hydroxide thermal decomposition produces MgO type products, including H_2O and HCl; water evaporation removes latent heat, which could reduce the plate surface temperature, inhibit material decomposition, and serve the function of dissolving a portion of harmful gases dissolved and delaying the fire (Yang and Li 2019). MgO itself is an excellent refractory material, such that the MgO coating of reed shavings effectively prevented the spread of flame (Figs. 9, 10).

Analysis of ignition time.—Ignition time (TTI) refers to the time taken by material from surface heating to surface continuous combustion and is used to evaluate and compare material fire resistance. Usually, the shorter the TTI, the easier the material ignites and the worse the fire resistance. The present test results showed that the TTI of inorganic particleboard was prolonged with increased sizing amount. At 50 percent, 55 percent, and 60 percent sizing, the inorganic particleboard TTIs were 361, 391, and 484 seconds, respectively.

Conclusions

(1) Sizing amount and density had the most significant effects on the performance of inorganic particleboard regarding fire retardancy and smoke suppression. The IB increased and TS decreased with increased sizing amount. With the increase in density, the MOR and MOE of reed inorganic particleboard increased, IB first increased and then decreased, and TS first decreased and then increased. The optimal technological parameters of this reed inorganic particleboard were 60 percent sizing capacity, 100°C hot-pressing temperature, 15 minutes hot-pressing time, and 1.2 g/cm^3 density. Under these conditions, the maximum values of plate MOR and MOE were 22.2 MPa and 3,608 MPa, respectively.

(2) The strength of this particleboard mainly derived from crystallization generated by hydration reactions. With increased sizing, the hydration reaction area increased and the greater crystallinity of hydration products led to better binding effects between the reed shavings and inorganic adhesive. When the sizing amount was 60 percent, hydration products were arranged more neatly and the peak diffraction intensity reached a maximum. At this point, hydration product crystallinity was also maximized and the mechanical strength maximized as well, so the particleboard demonstrated the best performance.

(3) This particleboard had excellent flame retardant and smoke suppression performance. With increased sizing amount, the HRR, SPR, and TSP all showed a downward trend, while the TTI was prolonged, indicating that the flame retardant and smoke suppression performance of this particleboard was significantly enhanced. Concurrently, $Mg(OH)_2$, MgO, H_2O, and other products produced by plate thermal decomposition increased, thus significantly improving flame retardant properties.

Literature Cited

Atoyebi, O. D., T. F. Awolusi, and I. E. E. Davies. 2018. Artificial neural network evaluation of cement-bonded particle board produced from red iron wood (*Lophira alata*) sawdust and palm kernel shell residues. *Case Stud. Constr. Mater*. 9:e00185.

Benthien, J. T., M. Ohlmeyer, M. Schneider, and T. Stehle. 2018. Experimental determination of the compression resistance of differently shaped wood particles as influencing parameter on wood-reduced particleboard manufacturing. *Eur. J. Wood Wood Prod.* 76:937–945.

Chen, M., X. Li, Y. Pan, Q. Tang and L. Zhu. 2016. Preparation and properties of inorganic poplar particleboard. *J. Compos. Mater.* 33(4):939–946.

Farag, E., M. Alshebani, W. Elhrari, A. Klash, and A. Shebani. 2019. Production of particleboard using olive stone waste for interior design. *J. Build. Eng.* 29. DOI:10.1016/j.jobe.2019.101119

Fu, B., X. Li, Y. Pan, X. Zheng, Y. Wu, and W. Zhong. 2015. Preparation and properties of inorganic wheat straw board. *Funct. Mater.* 46:1112–1116.

Fu, X. 2012. Preparation of phosphorus nitrogen boron flame retardant and its effect on the flame retardancy of particleboard. Master's dissertation. Chinese Academy of Forestry Sciences, Beijing, China.

Hafezi, S., A. Enayati, K. Hosseini, A. Tarmian, and S. Mirshokraii. 2016. Use of amino silane coupling agent to improve physical and mechanical properties of UF-bonded wheat straw (Triticum aestivum L.) poplar wood particleboard. *J. Forestry Res.* 27(2):427–431.

Hu, C., B. Xu, H. Ma, B. Chen, and Z. Li. 2016. Micromechanical investigation of magnesium oxychloride cement paste. *Constr. Build. Mater*. 105:496–502.

Huang, Q., X. Zhao, X. Zheng, and X. Li. 2008. Preparation and performance research of silicon magnesium cement bamboo particleboard. *New Build. Mater*. 45(9):25–29.

Lan, P., R. Huang, D. Zhou, and N. Brosse. 2015. Effects of inorganic composite flame retardants on flame retardancy of straw particleboard. *Forestry Sci. Technol. Dev*. 29(2):70–73.

National Standard of the People's Republic of China. 2009. Cement bonded particleboard. GB/ T 24312-2009. Nanjing, China.

Pang, L. and M. Yu. 2016. Preparation and application of flame retardant soybean protein adhesive. *China Adhes*. 25(9):34–37. (In Chinese with English abstract.)

Peng, S., C. Gui, X. Lin, C. Lan, and Z. Zhang. Study on technological parameters of bamboo particleboard prepared by soybean glue. *Forest Prod. Ind.* 2017, 44(9):19–23.

Widyorini, R., K. Umemura, R. Isnan, D. Putra, A. Awaludin, and T. Prayitno. 2016. Manufacture and properties of citric acid-bonded particleboard made from bamboo materials. *Eur. J. Wood Wood Prod.* 74:57–65.

Wang, X., Y. Deng, C. Liao, C. Chen, N. Wang, J. Wu, and T. Hou. 2013. Effects of reed stalk epidermis characteristics and water repellent dosage on particleboard performance. *J. Zhejiang Agric. Forestry Univ*. 30(2):245–250.

Wang, Z., L. Wang, D. Wu, and Z. Zhang. 2006. Research status and trend of reed in China. *Shandong Forestry Sci. Technol.* 6:85–87+74.

Xie, C. 2008. Research progress of magnesium hydroxide based flame retardants. *Nonferr. Mater. Eng*. 39(6):44–47+54.

Yang, K. and X. Li. 2019. Preparation of mineral bound particleboards with improved fire retardant and smoke suppression properties based on a mix of inorganic adhesive. *Holzforschung* 73(6). DOI:10.1515/hf-2018-0167

Zhang, H., J. Liu, Z. Wang, and X. Lu. 2013. Mechanical and thermal properties of small diameter original bamboo reinforced extruded particleboard. *Mater. Lett.* 100:204–206.

Zhang, J., A. Wu, and Y. Fu. 2015. Study on fiber morphology and characteristics of reed. *Pap. Papermak*. 34(6):55–58.

Zhang, X. 2012. Preparation of reactive magnesium oxide and study on expansion property of magnesium based cement. PhD dissertation.

Huazhong University of Science and Technology, Wuhan, Hubei province, China.
Zhou, Z., H. Chen, and Z. Li. 2015. Simulation of the properties of MgO-$MgCl_2$-H_2O system by thermodynamic method. *Cem*. *Concr. Res*. 68:105–111.
Zhu, X., Y. Wu, C. Tian, J.-M. Yang, and X. Zhang. 2015. Preparation technology and performance analysis of inorganic wheat straw board. *Forest Prod. Ind*. 42(6):18–22.
Zuo, Y., J. Xiao, J. Wang, W. Liu, X. Li, and Y. Wu. 2018. Preparation and characterization of fire retardant straw/magnesium cement composites with an organic-inorganic network structure. *Constr. Build*. *Mater*. 171:404–413.